Enhancement of Rail Track Performance through Utilisation of Geosynthetic Inclusions

Buddhima Indraratna[1], Sanjay Nimbalkar[2], and Cholachat Rujikiatkamjorn[3]
[1] *Professor of Civil Engineering and Research director, Centre for Geomechanics and Railway Engineering; Program Leader, ARC Centre of Excellence for Geotechnical Science and Engineering; University of Wollongong, Wollongong City, NSW 2522, Australia*
[2] *Research Fellow, Centre for Geomechanics and Railway Engineering; ARC Centre of Excellence for Geotechnical Science and Engineering; University of Wollongong, Wollongong City, NSW 2522, Australia*
[3]*Associate Professor, Centre for Geomechanics and Railway Engineering; ARC Centre of Excellence for Geotechnical Science and Engineering, University of Wollongong, Wollongong City, NSW 2522, Australia*
[1]*E-mail:* indra@uow.edu.au
[2]*E-mail*: sanjayn@uow.edu.au
[3]*E-mail*: cholacha@uow.edu.au

ABSTRACT: In coastal regions of Australia, high population density and increased traffic volumes have led to rapid expansion of rail transport. Use of artificial inclusions such as polymeric geosynthetics for enhanced soil-structure interaction and rubber shock mats for absorbing energy with the aim of reducing particle breakage is described in this paper as a cost-effective option. This paper highlights the results of a laboratory study on the deformation of coal fouled ballast stabilised with geogrids, at various degrees of fouling. A novel Track Process Simulation Apparatus (TPSA) was employed to reproduce realistic rail track conditions under cyclic loading, and the Void contaminant index (VCI) was used to assess the level of ballast fouling. The beneficial aspects of the geogrid inclusion are discussed in the paper. Laboratory results showed that biaxial geogrids can reduce the deformation of fresh ballast, but their effectiveness diminishes with an increase of VCI. A threshold value of VCI was proposed in view of track maintenance. Comprehensive field trials were executed on two full-scale rail tracks in the towns of Bulli and Singleton in New South Wales. These trials facilitated the evaluation of the relative performance of different types of geogrids, geocomposites and shock mats installed in fully instrumented track sections. Field trials showed that the use of recycled ballasted in rail tracks was a feasible and effective alternative. The performance of geogrids and geocomposite was found to be associated with their geometrical and mechanical properties as well as with the type of subgrade. The distributions of vertical and lateral stresses in the track were also assessed. In addition, effects of magnitude of axle load and train speed on stress distributions were studied.

Keywords: Railway Tracks; Deformation; Degradation; Geosynthetics; Ballast; Fouling

1. INTRODUCTION

In many countries, ballasted tracks are widely used because it is cost-effective and provides high load bearing capacity. In the past, most attention has been given to the track superstructure consisting of rails, fasteners and concrete sleepers (ties), and less attention to the substructure consisting of ballast, subballast (capping and structural-fill) and subgrade. Even though the substructure has a major influence on the cost of track maintenance, it has gained less attention because the properties of the substructure are more variable and difficult to define than those of the superstructure (Selig and Waters, 1994). With the increase in axle load, the interaction between the train and track has become more important in terms of design and analysis. Large cyclic loads from train passages can induce rapid deformations and degradation of the ballast layer (Lackenby et al., 2007; Anderson and Fair, 2008). Wheel-rail irregularities such as wheel flats, wheel shells, rail joints and rail corrugations can cause severe impact forces, thereby, accelerating the differential settlement and deterioration of the track components (Jenkins et al., 1974; Indraratna et al., 2011b).

Upon train loading, ballast deteriorates and becomes contaminated due to breakage and infiltration of fine particles into the void structure (e.g., coal fines, clay). Under typical Australian coal freight track conditions, Feldman and Nissen (2002) showed that coal fines make up 70-95% of the fouling materials. Han and Selig (1997); Tennakoon (2013) and Indraratna et al. (2013) investigated the effects of fouling on ballast settlement and demonstrated that settlement increases with an increasing degree of fouling. Tutumluer et al. (2008), Dombrow et al. (2009), and Huang et al. (2009) performed direct shear tests on fresh and fouled ballast at different degrees of fouling, and presented that coal dust can be considered the worst fouling material in view of reducing the shear strength.

Geosynthetics are often used to fulfill several functions in a new track construction or rehabilitation such as reinforcement, separation, filtration and drainage. If properly designed and installed, geosynthetics can improve the performance of rail tracks by increasing their serviceability and prolonging maintenance cycles. The benefits of geosynthetics in the stability improvement have been observed in several laboratory studies (Raymond, 2002; Indraratna and Salim, 2003; Indraratna et al., 2006, 2011a; Chen et al., 2012) and full-scale field trials (Ashpiz et al., 2002; Montanelli and Recalcati, 2003; Fernandes et al., 2008; Indraratna et al., 2010a). The effectiveness of geogrid reinforcement is highly dependent on the stiffness and size of the apertures (McDowell et al., 2006; Brown et al., 2007; Indraratna et al., 2011a) as well as the placement location (Bathurst and Raymond, 1987; Indraratna et al., 2007; Indraratna and Nimbalkar, 2013).

Installing shock mats in rail tracks can substantially attenuate the dynamic impact force. A shock mat is called an 'Under Ballast Mat' (UBM) when provided below the ballast layer, and an 'Under Sleeper Pad' (USP) when provided below the sleeper. The use of USPs to reduce dynamic stresses and vibrations (Esveld, 2009; Ferreira and López-Pita, 2013) and the use of UBMs to reduce ballast breakage (Indraratna et al., 2012a; Nimbalkar et al., 2012) have been studied earlier. However, the ballast-geosynthetic and ballast-USP/UBM interaction mechanisms can be very complex, depending on the type of the geosynthetics, the extent and type of ballast fouling, the conditions of the subgrade as well as the stress state in the real track environment. Considering the above, the relative performances of geogrids, geocomposite and shock mat under in-situ track conditions have been investigated during extensive field trials of instrumented track at Bulli and Singleton in the state of New South Wales (NSW), Australia.

2. BEHAVIOUR OF COAL FOULED BALLAST STABILISED WITH GEOGRID UNDER CYCLIC LOAD

2.1 Test Setup

In order to study the effects of geogrid and the influence of coal fines on the behaviour of fresh and fouled ballast, a series of large-scale triaxial tests employing the Track Process Simulation Apparatus (TPSA) was performed. The schematic cross section of the TPSA are shown in Figure 1. TPSA can accommodate a ballast assembly 800 mm long, 600 mm wide and 600 mm high. A cyclic load was applied by a servo-dynamic hydraulic actuator. The hydraulic jacks mounted on the sides of the apparatus are used to provide confining pressures in two horizontal directions (perpendicular and parallel to the sleeper). The load cells connected to hydraulic jacks are used to control the confining pressures to a prescribed range. The walls are rigid. The initial stresses were kept constant around 6-7 kPa in the transverse direction (parallel to sleeper), and about 10-12 kPa along the longitudinal direction (perpendicular to sleeper). The geogrid was always at the base of the ballast layer. This was done in accordance with current industry practice in Australia. The timber sleeper is 685 mm in length, 220 mm in width and 120 mm in height. All tests were performed on the fresh ballast and ballast mixed with coal at different degree of Void Contaminant Index (VCI) at a frequency of 15 Hz with a maximum cyclic pressure of 420 kPa, and tested up to 500,000 cycles. VCI, as proposed earlier by Indraratna et al. (2010b) and Tennakoon et al. (2012), has been adopted as follows:

$$VCI = \frac{1+e_f}{e_b} \times \frac{G_{sb}}{G_{sf}} \times \frac{M_f}{M_b} \times 100 \quad (1)$$

Where e_f = the void ratio of fouling material, e_b = the void ratio of fresh ballast, G_{sb} = the specific gravity of fresh ballast, G_{sf} = the specific gravity of fouling material, M_f = the dry mass of fouling material, and M_b = the dry mass of fresh ballast.

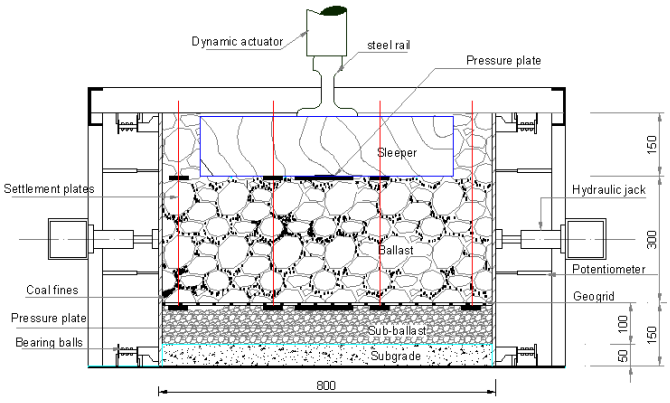

Figure 1 Schematic cross section of Rail Process Simulation Testing Apparatus (unit: mm) (Indraratna et al. 2013, © ASCE)

2.2 Test Results and Discussion

Figures 2a to 2d show the final values of ballast deformation and the relative deformation factor at 500,000 cycles with varying VCI. The relative deformation factor (R) can be calculated as follows:

Vertical settlement, S (%):

$$R_s = \frac{S_{(unreinforced)} - S_{(reinforced)}}{S_{(unreinforced)}} \times 100 \quad (2)$$

Lateral displacement, S_2 (%):

$$R_{h2} = \frac{S_{2(unreinforced)} - S_{2(reinforced)}}{S_{2(unreinforced)}} \times 100 \quad (3)$$

Lateral displacement, S_3 (%):

$$R_{h3} = \frac{S_{3(unreinforced)} - S_{3(reinforced)}}{S_{3(unreinforced)}} \times 100 \quad (4)$$

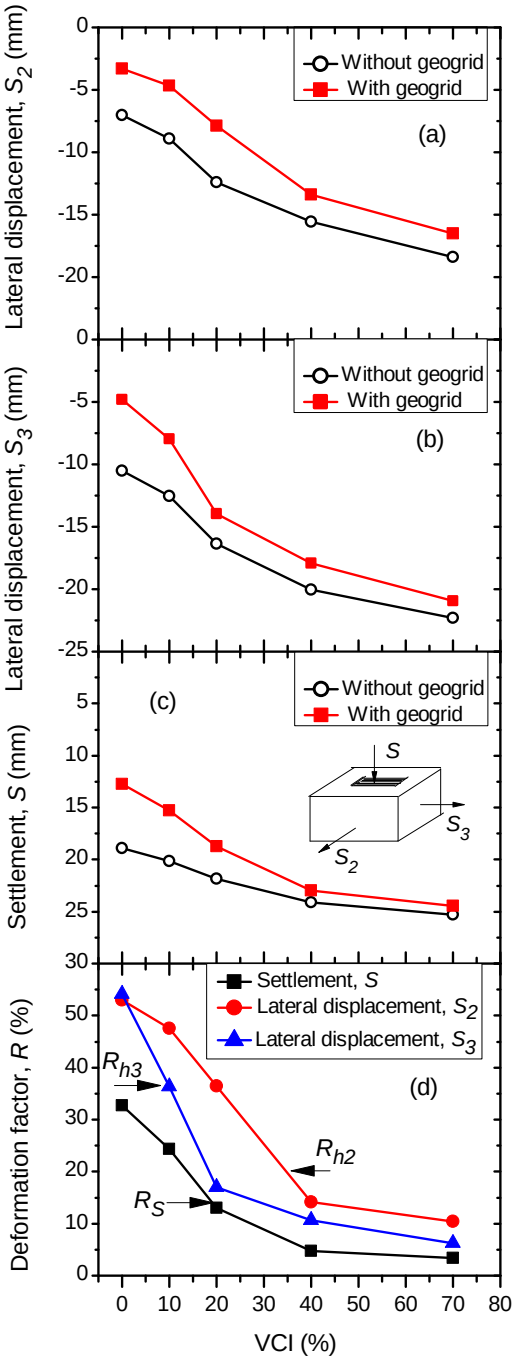

Figure 2 Variations of final deformation of fresh and fouled ballast with and without geogrid, with *VCI*: (a) lateral displacement S_2; (b) lateral displacement S_3; (c) settlement S; (d) ballast deformation factor, R (Indraratna et al. 2013, © ASCE)

The positive effect of geogrid on reducing ballast deformation is clearly revealed by the values of R presented in Figure 2d. The benefits of the geogrid reduced with an increase of VCI and became insignificant when VCI exceeded 40%. Geogrids can decrease the deformation of fresh ballast, but their effectiveness diminishes with an increase of VCI. At VCI = 40% and beyond, coal fines occupy

most of the ballast voids and geogrid apertures. This phenomenon prevents the ballast particles from effectively interlocking with the geogrid. A threshold value of VCI = 40% is proposed as a limiting value where the effect of geogrid becomes marginal and track maintenance would become essential.

3. FIELD STUDY AT BULLI

In order to study the benefits of using geosynthetics in fresh and recycled ballast and to examine the performance of recycled ballast as a cheaper and feasible technical alternative to the use of more expensive fresh ballast, a field trial was undertaken on a section of instrumented track at Bulli, NSW (Indraratna et al., 2010a).

3.1 Site Geology

About 8 test pits and 8 electrical friction cone penetrometer tests were carried out as a part of site investigation to assess the subsurface conditions. The subgrade was stiff over-consolidated silty clay. The bedrock was highly weathered sandstone and was located at about 2.8 m below the ground level.

3.2 Track Construction

A 60 m long section of instrumented track located between two turnouts at Bulli, part of RailCorp's South Coast Track was selected for this field trial. The instrumented track section was divided into four equal Sections. Fresh and recycled ballast was used at Sections 1 and 4, respectively, without the inclusion of a geocomposite layer, while Sections 2 and 3 were built by placing a geocomposite layer at the base of the fresh and recycled ballast, respectively. The overall granular layer thickness was 450 mm including a ballast layer of 300 mm and a capping layer of 150 mm in thickness. A layer of geocomposite (combination of biaxial geogrid and nonwoven polypropylene geotextile) was placed at the ballast-capping interface.

3.3 Material Specifications

The fresh ballast was obtained from Bombo quarry (NSW) and represented sharp angular coarse aggregates of crushed volcanic (latite) basalt, and its particle gradation was in accordance with the Technical Specification TS 3402 (RailCorp, Sydney). Recycled ballast was collected from spoil stockpiles at Chullora yard near Sydney. The waste ballast was removed from the deteriorated track during the maintenance. The physical examination indicated that about 90 % of the recycled ballast comprised of semi-angular crushed rock fragments, while the remaining 10 % consisted of semi-rounded river gravels and other impurities (sleeper fragments, cemented materials, etc.). The recycled ballast was cleaned and sieved to remove the finest fraction (less than 9.5 mm). The capping was a mixture of sand and gravel. The particle size distributions of fresh ballast, recycled ballast, and capping materials are given in Table 1.

Table 1 Grain size characteristics of fresh ballast, recycled ballast and capping (data sourced from Indraratna et al., 2010a, © ASCE)

Material	d_{max} mm	d_{min} mm	d_{50} mm	C_u	C_c
Fresh Ballast	75.0	19.0	35.0	1.5	1.0
Recycled Ballast	75.0	9.5	38.0	1.8	1.0
Capping	19.0	0.05	0.26	5.0	1.2

The values of coefficient of uniformity, C_u (= d_{60}/d_{10}, where d_{60} is the particle size at 60% passing and d_{10} is the particle size at 10% passing) and coefficient of curvature, C_c (= $d_{30}^2/d_{10}\times d_{60}$, where d_{30} is the particle size at 30% passing) are also shown for comparison. The technical specifications of the geocomposite layer are shown in Table 2. The values are indicated as MD × TD; where MD is machine direction (longitudinal to the roll) and TD is transverse direction (across the roll width).

Table 2 Mechanical properties of geocomposite

Characteristics	Unit	Data
Biaxial geogrid		
Tensile strength	kN/m	30 × 30
Strain at break	%	11 × 10
Aperture size	mm	40 × 27
Thickness	mm	2
Mass per unit area	g/m^2	420
Nonwoven geotextile		
Thickness	mm	2
Mass per unit area	g/m^2	140

3.4 Track Instrumentation

The behaviour of the experimental track section was monitored using sophisticated instruments. Thin pressure cells with semiconductor type transducers were used to record the vertical and horizontal stresses. Relatively thin pressure cells (thickness of 12 mm, diameter of 230 mm) were used. The horizontal pressure cells were installed at the sleeper-ballast, ballast-capping, and capping-subgrade interfaces, and vertical pressure cells were used at sleeper-ballast and ballast-capping interfaces (Indraratna et al., 2010a). Vertical and lateral deformations were measured using settlement pegs and electronic displacement transducers, respectively.

Although, the use of displacement transducers to measure vertical displacements is quite common in practice, they were used to record transient lateral track displacements in this study. This is because, under a normal rail track, significant lateral displacements occur in the ballast which in turn affects the track stability. These transducers (also known as extensometers) were placed inside two, 2.5 m long stainless steel tubes that can slide over each other, with 100 mm × 100 mm end caps as anchors with a capacity to measure upto 150 mm displacements. The settlement pegs consisted of 100 mm × 100 mm × 6 mm stainless steel base plates attached to 10 mm diameter steel rods. The settlement pegs and displacement transducers were installed at sleeper-ballast and ballast-capping interfaces, as shown in Figure 3. Pressure cells and displacement transducers were connected to an automatic data acquisition (DAQ) system in order to obtain real time data.

3.5 Track Measurements

A relationship between the total traffic in million gross tons (MGT) and axle load (A_t) was used to determine the number of load cycles (Selig and Waters, 1994):

$$N = \frac{T}{A_t \times N_a} \tag{5}$$

where N = the number of load cycles; A_t = the axle load in tons; and N_a = the number of axles per load cycle. The railroad car passes are preferred over the number of axle passes because the wheels of adjacent bogies have been always found to overlap each other (Indraratna et al. 2010a, 2012a). In this study, T = 60 MGT, N_a = 4 and A_t = 25 tons are considered as best estimates of traffic accumulated during the course of measurements. Substituting these input parameters, about 600,000 load cycles per year are calculated using Eq. (5). Therefore the results were plotted against the number of load cycles, as discussed below.

Figure 3 Installation of settlement pegs and displacement transducers in experimental sections of track at Bulli

3.5.1 Traffic induced peak stresses in ballast

One of the objectives of this field trial was to assess distribution of vertical and lateral stresses in the track. In addition, effect of magnitude of axle load on stress distributions was studied. For the laboratory testing purpose, elastic analysis using conventional methods was conducted to obtain vertical stresses. Table 3 shows the maximum vertical cyclic stresses (σ_v') and maximum horizontal cyclic stresses (σ_h') recorded in Section 1 (i.e. fresh ballast). These stresses were measured during the passage of passenger train (20.5 ton axle load) and coal freight train (25 ton axle load) travelling at 60 km/h. As expected, the maximum cyclic stresses (σ_v', σ_h') measured in the layer of ballast and capping were higher for a coal freight train than a passenger train. It was thus apparent that a greater axle load imposed a higher σ_v' and σ_h' which resulted in increased deformation and degradation of the ballast, implying the need for earlier track maintenance. The larger σ_v' and relatively smaller σ_h' caused significantly large shear strains in the track. Track confinement (σ_h') can be increased by reducing the spacing of sleepers, increasing the height of shoulder ballast, placing a geosynthetic layer at the ballast-subballast interface, widening the sleepers at both ends, and using intermittent lateral restraints at various parts of the track (Lackenby et al., 2007).

Table 3 Maximum cyclic stresses measured under the rails (σ_v', σ_h') (data sourced from Indraratna et al., 2010a, © ASCE)

Axle load	**A_t = 20.5 tons**		**A_t = 25 tons**	
Stresses (kPa)	**Vertical (σ_v')**	**Lateral (σ_h')**	**Vertical (σ_v')**	**Lateral (σ_h')**
Sleeper-ballast	238	25	293	46
Ballast-capping	63	18	86	26

The DAQ unit used in the Bulli field trial could operate at a maximum frequency of 40 Hz. For a train speed of 60 km/h, a wheel could travel a distance of 0.4 m in 1/40th of a second, and therefore it could not be ascertained that any wheel would be over the instrumented sleeper at the time of recording.

3.5.2 Vertical and lateral strains

Track settlement occurs in two major phases (Dahlberg, 2006). The first phase occurs directly after tamping, when the track position is adjusted to a straight level, the settlement is relatively fast until the gaps between the ballast particles are reduced and the ballast is compacted (e.g. Selig and Waters, 1994; Aursudkij, 2007; Fischer and Horv′at, 2011). The second phase of settlement is slower and there is a non-linear relationship between settlement and time (or number of load cycles). The second phase of settlement is caused by the densification and inelastic behaviour of ballast, subballast (capping and structural fill), and subgrade materials. In this study, although these two phases are not shown distinctly, the cumulative effect of both resulted in the overall deformations reported herein.

Under repeated loading, the ballast layer undergoes compression in the vertical direction and expands in the two lateral directions. However, lateral deformations perpendicular to sleepers are usually very small due to the higher level of longitudinal restraint offered by the rail-sleeper assembly, hence neglected in the current study. The vertical and lateral deformations (S_v, S_h) of ballast were determined by subtracting displacements of the ballast-capping interface from those at the sleeper-ballast interface. The mean vertical strain (ε_v) is defined as the ratio of S_v to the initial ballast thickness (i.e. 0.3 m). The mean lateral strain (ε_h) is defined as the ratio of S_h to the initial lateral dimension (considered as 2.5 m) of the ballast layer. The mean vertical and lateral strains (ε_v, ε_h) are plotted against the number of load cycles (N) in Figures 4a and 4b, respectively. The vertical strain is highly non-linear under cyclic loading and its non-linear variation against the number of load applications is best described by a semi-logarithmic relationship (Brown and Selig, 1991; Raymond and Bathurst, 1994; Indraratna et al., 2011b) such as:

$$\varepsilon_v = a' + b' \left(\ln N \right) \tag{6}$$

where, a' and b' are two empirical constants, depending on the type of ballast, type of geosynthetics used, and the initial placement density. The non-linear variation of ε_v with increasing load cycles becomes linear in the semi-logarithmic plot (Figure 4a). When the results obtained from Sections 1 and 2 are compared, the vertical strain of ballast with geosynthetics is found to be about 40% smaller than that without reinforcement (Figure 4a). The similar trend is observed also in the laboratory (Shin et al., 2002; Indraratna and Salim, 2003; Brown et al., 2007; Indraratna and Nimbalkar, 2013), and is mainly attributed to the interlocking between ballast particles and the grid apertures, thus creating an enhanced track confinement. Similarly, the relationship between the mean lateral strain of ballast and the logarithm of load cycles can be expressed by:

$$\varepsilon_h = c' + d' \left(\ln N \right) \tag{7}$$

where, c' and d' are two empirical constants. The values of empirical constants (a', b', c', d') are obtained by performing a linear regression analysis and are shown in Figures 4a and 4b. These results reveal that fresh ballast stabilised with geocomposite exhibited less lateral strain (ε_h) than fresh ballast (without any geosynthetics) at a higher number of load cycles. This result has a significant bearing in the maintenance of rail tracks because reducing the lateral movement of ballast with the inclusion of geocomposites implies a reduced need for additional crib and shoulder ballast during maintenance.

The recycled ballast showed improved performance, i.e. less vertical and lateral strains, because of its moderately graded particle size distribution (C_u = 1.8) compared to the highly uniform fresh ballast (C_u = 1.5). If a layer of fresh ballast is replaced with a layer of moderately graded recycled ballast, the corners of individual particles will not break as frequently as highly angular particles of fresh ballast. However, the recycled ballast exhibited larger vertical and lateral strains when reinforced with geogrid. The mean particle

size (d_{50} = 38 mm,) of recycled ballast was larger than that of the fresh ballast (d_{50} = 35 mm). Thus, the fresh ballast had a better interlocking effect with the geogrid aperture size of 40 × 27 mm.

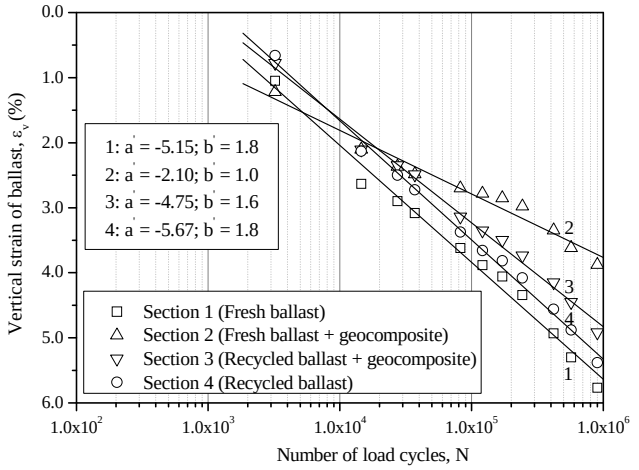

(a)

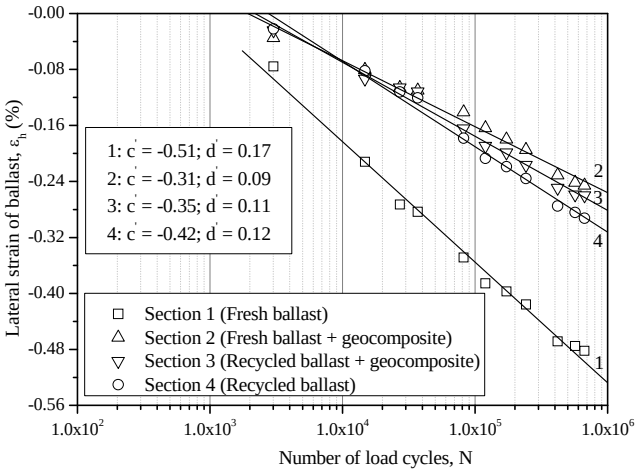

(b)

Figure 4 (a) vertical and (b) lateral strains of the ballast layer plotted in semi-logarithmic scale (data sourced from Indraratna et al., 2010a, © ASCE)

The results of the field trial demonstrated the potential benefits of using a geocomposite at the base of the ballast layer in track, where it was able to reduce the vertical strain of fresh ballast by 33% and that of recycled ballast by 9%. It also reduced the lateral strain of fresh ballast by about 49% and that of recycled ballast by about 11%. The apertures of the geocomposite offered a strong mechanical interlock with the ballast, forming a highly frictional interface. The ability of geosynthetics to reduce the rate of track deterioration would be appealing to the railway industry because the cost of installation is relatively lower compared to the substantial benefits generated by an extended life span, and more resilient track performance.

4. FIELD STUDY AT SINGLETON

To investigate effectiveness of different types of geosynthetics and UBMs to improve the overall stability of the track under in situ conditions, an extensive study was undertaken on fully instrumented sections of track near Singleton, NSW. The key influential factors, i.e., the stiffness, aperture size, and filtration ability of geosynthetics under 'field' conditions were investigated. The use of energy absorbing UBMs in order to minimise any degradation of the ballast at the concrete bridge deck was also studied.

4.1 Site Geology

An extensive program of sub-surface exploration (33 bore holes and 107 test pits) indicated that the track was located on a massive sedimentary outcrop of rock, between 224.20 and 229.00 km, and later on the flood plain of the Hunter River (RCA Australia 2008). The rock outcrop was part of the Branxton Formation and mainly composed of medium to high strength siltstone. The flood plain consisted of a layer of an alluvial deposit of silty clay 7-10 m thick, underlain by heterogeneous layers of medium dense sand and silty clay with a total thickness of 7-9 m. Medium strength siltstone was found beneath the layer of sand and silty clay.

4.2 Track Construction

A 10.86 km long section of instrumented track located between the towns of Bedford (chainage 224.20 km) and Singleton (chainage 235.06 km) in New South Wales was selected for this field trial. Eight experimental sections located on three different types of sub-grades, including (i) the relatively soft general fill and alluvial silty clay deposit (Sections 1-4 and Section A), (ii) the intermediate cut siltstone (Sections 5 and C), and (iii) the stiff reinforced concrete bridge deck supported by a piled abutment (Section B) were considered as a part of this study. A 300 mm thick layer of ballast was underlain by a 150-300 mm thick capping layer. A structural-fill layer with a maximum of 600 mm thickness was placed below the capping. Different types of geosynthetics were installed in a single layer at the ballast-capping interface. For comparison purposes, no geosynthetic was installed at Sections A and C. A layer of UBM was installed between the ballast and bridge deck at Section B.

4.3 Material Specifications

The ballast consisted of angular latite basalt rock and was obtained from a quarry near Singleton. The capping and structural-fill was compacted sandy gravel and was also obtained from the same quarry. The particle size distributions of the ballast, capping and structural-fill were in accordance with industry practices (ARTC, 2006a, b; 2007a, b). The gradation and USCS classification of these materials are reported in Table 4.

Table 4 Gradation characteristics and USCS classification of ballast, capping, and structural-fill

Material	Description	d_{50} (mm)	USCS classification	*CBR* (%)
Ballast	Compacted angular latite	36	GP	-
Capping	Compacted sandy gravel	4	GP-GM	50
Structural-fill	Compacted sandy gravel	3	GP-GM	30

Three commercially available biaxial geogrids (GG1, GG2, GG3) and one geocomposite (GC) which is a combination of biaxial geogrid and non-woven polypropylene geotextile, were used in the present study. Their physical and mechanical characteristics are listed in Table 5. The UBM was made of recycled rubber granulates of 1-3 mm sizes bounded by polyurethane elastomer compound. Table 6 shows the relevant properties of the UBM.

Geogrids GG1, GG2 and geocomposite GC were installed at Sections 1, 2 and 4 respectively. The geogrid GG3 was used at Sections 3 and 5. The UBM layer was placed at Section B. Sections A and C consisted of fresh ballast without any geosynthetic or UBM.

Pressure cells and settlement pegs were used to measure traffic induced vertical stresses and vertical deformations of the ballast layer, respectively. Technical specifications of the equipment were similar to those used during the field trial at Bulli.

Table 5 Mechanical properties of geogrids and geocomposite

Material	GG1	GG2	GG3	GC	
Type		biaxial		biaxial	Nonwoven
Tensile stiffness (MN/m)	1.8×1.8	1.5×1.5	1.5×1.5	2.0×2.0	0.3×0.5
Tensile strength (kN/m)	36×36	30×30	30×30	40×40	6×10
Strain at break (%)	15×15	15×15	15×15	15×15	60×40
Aperture size (mm)	44×44	65×65	40×40	31×31	-
Thickness (mm)	3	3	4	3	2.9

Table 6 Mechanical properties of shock mat (UBM)

Characteristics	Unit	Data
Particle size	mm	1-3
Young's modulus	MPa	6.12
Tensile strength	kN/m^2	600
Strain at break	%	80
Thickness	mm	10

4.4 Track Instrumentation

Pressure cells and settlement pegs were used to measure traffic induced vertical stresses and vertical deformations of the ballast layer, respectively. Technical specifications of the equipment were similar to those used during the field trial at Bulli. Two pressure cells were installed at Sections 1, 5, A, and C, one below the sleepers and the other below the layer of load bearing ballast. At Section B, three pressure cells were installed between the synthetic mat and the deck. Two pressure cells were located below the up rail, while another was placed below the down rail. Settlement pegs were installed between the sleeper and ballast and between the ballast and capping to measure the vertical deformation of ballast.

In addition, strain gauges and transient displacement monitoring frame were used during this field trial. The strain gauges were a post yield type suitable to measure tensile strains between 0.1 to 15%. They were installed in a group, about 200 mm apart, at the top and bottom sides of the grids, in both longitudinal and transverse directions. At each section, one group of strain gauges was installed below the edge of the sleeper, while another was below the up rail. Protective layers made of vulcanized rubber were used to cover the strain gauges to minimise any damage caused by contact with the ballast. Flexible aluminium sleeves were also used to protect the data cables against damage from sharp ballast aggregates, as shown in Figure 5.

Transient deformations of the ballast layer were measured by five potentiometers (POTs) mounted on a custom built aluminum frame, as shown in Figure 6. The two POTs were mounted vertically on the frame, one to monitor movement of the sleepers, and the other to measure the movement of settlement peg placed at top of the capping. The other three POTs were mounted in an inclined fashion to monitor the vertical and horizontal deformations of the 'shoulder ballast' at different locations. The deformation frame was held in place by support bases installed in the capping and layers of structural-fill.

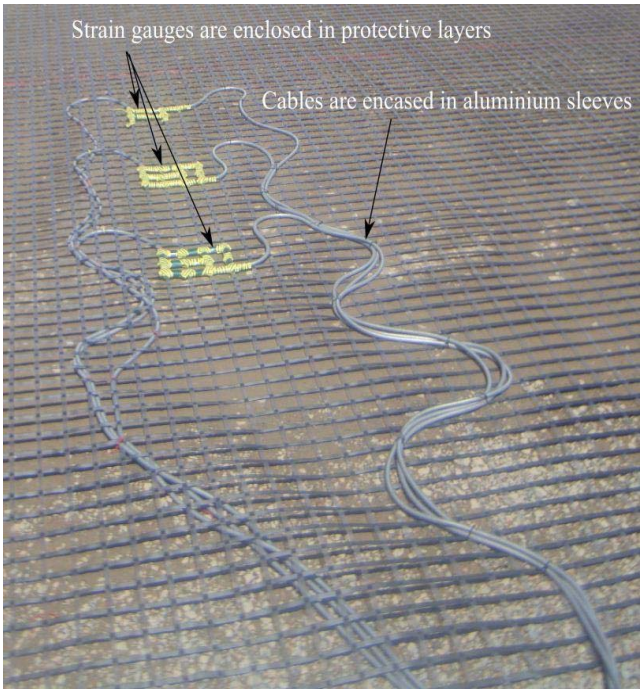

Figure 5 Placement details of instrumented strain gauges

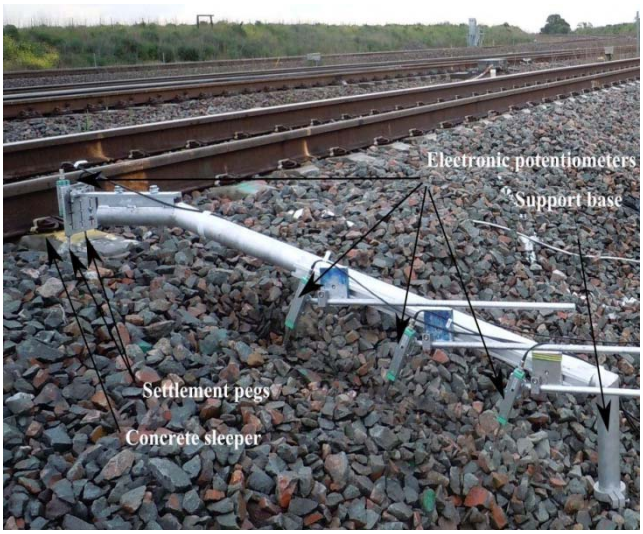

Figure 6 Displacement monitoring frame mounted on support base

Electrical analogue signals from the strain gauges, pressure cells, and potentiometers were obtained using a mobile DAQ unit. Considering the limitations associated with low frequency data as discussed earlier, much advanced DAQ unit was used in this field trial to obtain data from the aforementioned instruments at a frequency of 2000 Hz. The input signals were amplified and filtered to reduce signal noises.

4.5 Track Measurements

The vertical strains of ballast and irrecoverable strains in geosynthetics were measured against time. More appropriate scale of 'number of load cycles' is necessary in lieu of the 'time' scale. Considering T = 64 MGT, N_a = 4, A_t = 25 and 30 tons as best estimates of train traffic during the period of measurements and using Eq. (5), about 330,000 load cycles are considered.

4.5.1 Traffic induced vertical stresses

The maximum vertical cyclic stresses (σ_v') recorded in Section C (i.e. fresh ballast) are shown in Table 7. These stresses were measured during the passage of coal freight trains (axle load of 25 and 30 tons) travelling at 40 km/h and 60 km/h. As anticipated, the maximum vertical stresses (σ_v') measured at the ballast-capping interfaces were significantly lower (about four-fold) than those at sleeper-ballast interfaces. This elucidates the role of the ballast layer for effective dissipation of stresses with depth. The vertical stresses (σ_v') due to passage of coal freight train (axle load of 25 tons) travelling at 60 km/h were quite larger than those measured during the Bulli field trial. While Authors acknowledge the limitations of a direct comparison owing to variations in track substructure conditions, the data recording at higher frequency certainly offered more reliable estimation of maximum stresses from the wheel load. As expected, the greater axle load induced a higher σ_v'. It was also found that higher train speeds increased the stresses at the sleeper-ballast and ballast-capping interfaces. This finding is in agreement with other studies in the past (Shenton, 1975; Jeffs and Tew, 1991; Kempfert and Hu, 1999). The effect of increased train speed was more pronounced at the sleeper-ballast interface. This study clearly highlights the implications of the increased train speeds on the ballast contact stresses.

Table 7 Vertical cyclic stresses measured under the rail (σ_v')

Axle load (tons)	A_t **= 25**		A_t **= 30**	
Speed, V (km/h)	40	60	40	60
Sleeper-ballast	290	301	315	338
Ballast-capping	85	89	94	102

4.5.2 Vertical strains of ballast

The relationship between ballast strains and the number of load cycles (N) is usually non-linear. Therefore vertical strain (ε_v) of the ballast is plotted against the number of load cycles (N) in a semi-logarithmic scale as shown in Figures 7a and 7b. Using the linear relationship defined using Eq. (6), the values of empirical constants a' and b' are obtained by performing a linear regression analysis (Figures 7a and 7b). When the results for sections on similar subgrades were compared, vertical strains of the geogrid-reinforced sections (i.e. Sections 1 and 2) were 10-32% smaller than that of fresh ballast without reinforcement (i.e. Section A). The use of geocomposite layer also reduced the ballast strains by about 28%.

When the results for sections with similar geogrids are compared (i.e. Section 3 and Section 5), it is apparent that the reinforcement ability of geogrid to reduce track settlement is generally higher for softer subgrade (low track substructure stiffness). Such an observation is in agreement with the results of the full scale laboratory tests presented elsewhere by Ashmawy and Bourdeau (1995). The geogrid GG3 performed better compared to other geogrid types (e.g. GG1 and GG2). Although the tensile stiffness of GG3 is very similar to others (Table 5), its aperture size of 40 mm enabled better interlocking between the ballast particles and grids. This finding also agrees with the criteria for optimum size apertures for geogrids proposed by Brown et al. (2007) and Indraratna et al. (2011a).

4.5.3 Transient strains developed in ballast

Transient deformations of the ballast layer were measured using the deformation frame. It was observed that the passage of trains with an axial load of 30 tons travelling at 40 km/h resulted in a vertical deformation (S_{tv}) between 1.5 to 3.0 mm, resulting in average vertical strain (ε_{tv}) of between 0.5 and 1.0%. The transient horizontal deformations (S_{th}) measured on the surface of shoulder ballast (up rail side) were all dilative and between 0.5 to 0.3 mm outward from the track centreline. This resulted in an average horizontal strain (ε_{th}) of -0.05 to -0.02%. The horizontal strains were larger near the crest and smaller near the toe of ballast. The average transient strains (ε_{tv} , ε_{th}) in the ballast layer with reinforcement were about 15% smaller than those without reinforcement.

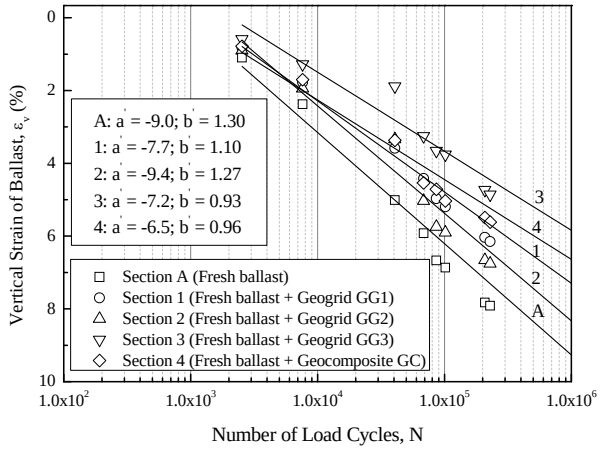

(a)

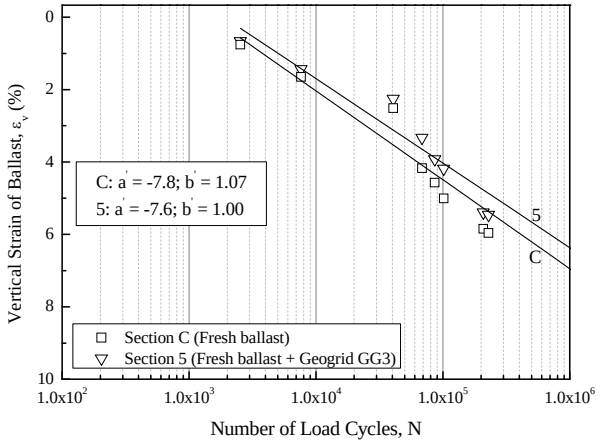

(b)

Figure 7 Vertical strains of ballast layer plotted versus number of load cycles in semi-logarithmic scale for (a) soft embankment; and (b) hard rock

4.5.4 Irrecoverable and transient strains in geosynthetics

Irrecoverable (long-term) longitudinal (ε_l) and transverse (ε_t) strains measured from strain gauges installed below the edges of sleepers are given in Figure 8. It is observed that most strains (ε_l, ε_t) were developed in the geogrids when the track was being constructed, particularly when the ballast was being placed. In general, these strains (ε_l , ε_t) increased with the number of load cycles. The transverse strains were generally larger than the longitudinal strains, probably due to confinement or a higher level of longitudinal restraint relative to the transverse direction. The transverse strains (ε_t) developed in the geocomposite (i.e. GC at Section 4) were relatively large. This is because the railway embankment underwent large lateral deformation shortly after the track was commissioned. The strains accumulated in the geosynthetics were influenced by the placement of ballast and deformation of the subgrade.

Induced transient strains in geosynthetics along both the longitudinal (ε_{tl}) and transverse (ε_{tt}) directions were between 0.14-0.17%. These strains were measured during the passage of freight trains with an axial load of 30 tons travelling at 40 km/h. The comprehensive information on the variation of transient strains with the number of load cycles is not available as the field monitoring is currently ongoing. The induced transient strains were mainly affected by the stiffness of the geogrids.

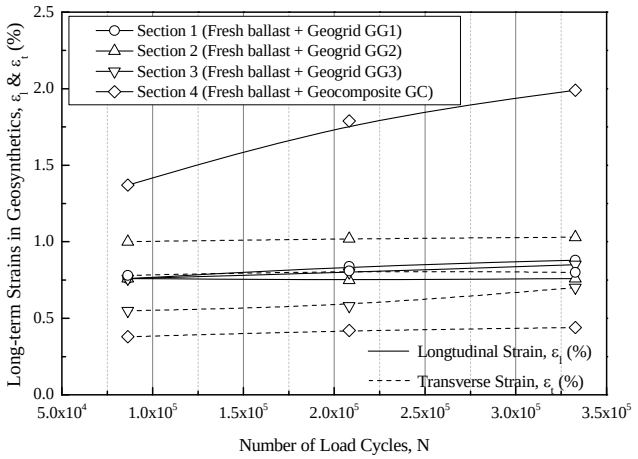

Figure 8 Strains accumulated in geogrids and geocomposite in transverse and longitudinal directions versus number of load cycles

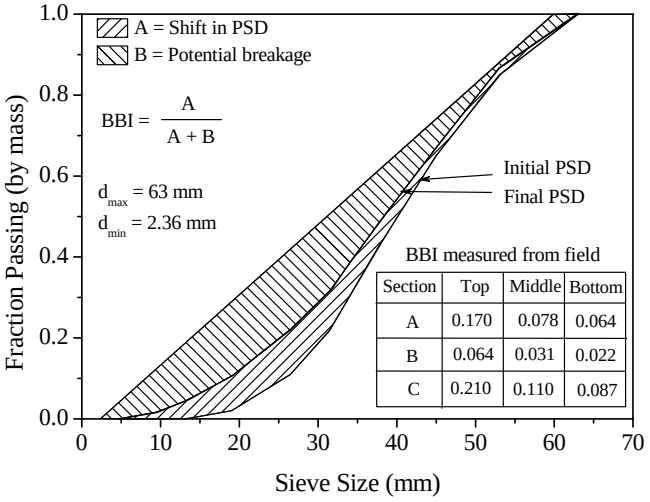

Figure 9 Determination of ballast breakage index (data sourced from Indraratna et al., 2005)

4.5.5 Ballast breakage

Samples were recovered from load bearing ballast in order to assess the particle degradation subjected to train traffic loading (780,000 load cycles). A sampling pit with plan area of about 1.8 m × 1.3 m was formed by excavating the ballast from the crib, shoulder and load bearing segments of the rail track. Samples were recovered from three equal portions between the bottom of sleeper and formation level in order to assess the variation of ballast breakage with depth. Samples of ballast were obtained in accordance with AS 1141.3.1 (2012). A proper care was taken to collect fine particles trapped inside voids of ballast. The ballast profile was then reinstated using clean ballast and tamped using a tamping head on the excavator. Small containers were used to avoid segregation during the transport to the laboratory following the approach by Feldman and Nissen (2002). The separation of samples collected from three equal portions of load bearing ballast also enabled the assessment of the variation of ballast breakage with depth. Visual inspection of the samples showed only rock fragments which most likely resulted from particle breakage. Ballast was relatively clean with no evidence of fouling due to spillage of coal from passing trains and 'slurry pumping' of the fines from the underlying subgrade. The breakage is quantified using the parameter, Ballast Breakage Index (BBI), proposed by Indraratna et al. (2005). As shown in Figure 9, BBI was determined by using a linear hypothetical size axis as reference.

The value of ballast breakage index (BBI) for Sections A, B and C are also shown in Figure 9. As expected, the ballast breakage was highest at the top and decreased with depth. The variations in the BBI with depth were found quite similar to those observed in stresses and displacements of load bearing ballast layer. Largest values of BBI at Section C revealed that particle breakage was influenced by the type of subgrade. The particle degradation phenomenon is more pronounced for stiff subgrade than that for the relatively soft or weak subgrade (Indraratna et al., 2012b; Nimbalkar et al., 2012).

It is also interesting that this result is in agreement with measurements related to track transition zone previously reported by Li and Davis (2005). In practice, the sleeper on the approach between soft and stiff subgrade has largest settlement, which imply most particle breakage. Although the track support conditions at Section B (concrete bridge) are much stiffer than those at Section A (alluvial silty clay deposit), larger lateral confinement from the barriers of Mudies Creek bridge most likely resulted in a significantly smaller value of BBI. These results may also suggest the effectiveness of UBMs in reducing ballast degradation when placed above the concrete deck. However, this warrants sufficient data from a similar bridge without any UBM for further validation.

5. CONCLUSIONS

A comprehensive field monitoring program was undertaken at the towns of Bulli and Singleton in NSW, Australia, to study the ability of various geosynthetics types and shock mats to improve the overall stability of ballasted rail tracks. The sophisticated instrumentation schemes used during these field trials have led to a significant understanding of the stress-strain and degradation mechanisms in the ballasted track. A series of laboratory tests of ballast at different void contaminant index with and without geogrid were performed to study the geotechnical behaviour of coal fouled ballast using the Track Process Simulation Testing Apparatus. Based on the test results, while the geogrid reduces the deformation of ballast due to effective interlocking occurring at the ballast geogrid interface, coal fines increase the ballast deformation. Geogrid was more useful at reducing the breakage of ballast when the VCI was less than 40%, but beyond that its effect was found to be negligible.

The results of the Bulli study indicated that the use of recycled ballasted in rail tracks proved to be a feasible and effective alternative. This was due to a composition of moderately graded recycled ballast that interlocked within the granular assembly much more effectively than the highly uniform fresh ballast recommended by the Australian Standards. The results also demonstrated the potential benefits of using geocomposite as reinforcing elements in track, where it was able to reduce the vertical strain of fresh ballast by about 33% and that of recycled ballast by about 9%. It also reduced the lateral strain of fresh ballast by about 49% and that of recycled ballast by about 11%. The apertures of the geogrid component of geocomposite offered a strong mechanical interlock with the ballast, forming a highly frictional interface. The geocomposite was effective in providing the key functions of reinforcement, and filtration and separation, thereby reducing the vertical and lateral deformations. Effect of magnitude of axle load on the distribution of vertical and lateral stresses in the track was also studied. It was found that vertical and lateral stresses increased with magnitude of axle load.

The results of the Singleton study showed that the performance of geogrids and geocomposite is governed by their geometrical and mechanical properties as well as by the type of subgrade. Three types of biaxial geogrids and one geocomposite (combination of biaxial geogrid and non-woven polypropylene geotextile) were installed at the ballast-capping interface. The experimental track sections were located on different types of subgrades. It was found that geogrids and geocomposite could decrease the vertical strains of ballast as much as 35%, with obvious benefits of improved track stability and decreased maintenance cost. The aperture size of the

geogrid which resulted in the least ballast deformation (both long-term and transient) was in the range of $1.1d_{50}$. The use of geosynthetics was found to be more effective in track sections located on the softer subgrade. The irrecoverable strains in the geosynthetics were influenced by the placement of the ballast and deformation of the subgrade, while the induced transient strains were mainly affected by the stiffness of the geogrids. The traffic-induced vertical stresses at the ballast-capping interface were larger on stiffer subgrades. It was found that high train speeds would increase the dynamic forces and impart greater stresses on the ballast. The reduced ballast breakage at the concrete bridge could be attributed to increased lateral confinement. The use of shock mat (UBM) could also lead to the reduced ballast breakage. However, this needs further validation through more field data from a similar bridge without any UBM.

6. LIST OF NOTATIONS

a', b'	Empirical constants relating vertical strain and the logarithm of number of load cycles
A_t	Axle load (tonne)
c', d'	Empirical constants relating lateral strain and the logarithm of number of load cycles
C_c	Coefficient of curvature
C_u	Coefficient of uniformity
d_{50}	Particle size at percent finer of 50% (mm)
d_{max}	Maximum particle size (mm)
d_{min}	Minimum particle size (mm)
e_b	Void ratio of fresh ballast
e_f	Void ratio of fouling material
GC	Geocomposite placed at Section 4
GG1	Biaxial polypropylene geogrid placed at Section 1
GG2	Biaxial polypropylene geogrid placed at Section 2
GG3	Biaxial polypropylene geogrid placed at Sections 3 and 5
GM	Poorly graded silt
GP	Poorly graded gravel
G_{sb}	Specific gravity of ballast
G_{sf}	Specific gravity of fouling material
MD	Machine direction (longitudinal to the roll)
M_f	Dry mass of fouling material (kg)
M_b	Dry mass of fresh ballast (kg)
N	Number of load cycles
N_a	Number of axles per load cycle
R	Relative deformation factor
S	Vertical settlement of ballast (mm)
S_2	Lateral displacement of ballast parallel to rail (mm)
S_3	Lateral displacement of ballast parallel to sleeper (mm)
S_h	Horizontal deformation of ballast layer (mm)
S_{th}	Transient horizontal deformation of ballast layer (mm)
S_{tv}	Transient vertical deformation of ballast layer (mm)
S_v	Vertical deformation of ballast layer (mm)
T	Total traffic tonnage (tonne)
TD	Transverse direction (across the roll width)
V	Train speed (km/h)
BBI	Ballast breakage index
CBR	California Bearing Ratio (%)
DAQ	Data acquisition system
MGT	Million gross tonnes of traffic
POT	Electronic potentiometer
PSD	Particle size distribution
VCI	Void contaminant index
UBM	Under ballast mat (shock mat)
USP	Under sleeper pad (shock mat)
USCS	Unified Soil Classification System
σ'_h	Traffic-induced horizontal stress (kPa)
σ'_v	Traffic-induced vertical stress (kPa)
ε_h	Horizontal (lateral) strain of ballast layer (%)
ε_l	Cumulative longitudinal strain in geosynthetics (%)
ε_t	Cumulative transverse strain in geosynthetics (%)
ε_{th}	Transient average horizontal strain of ballast layer (%)
ε_{tl}	Transient longitudinal strain in geosynthetics (%)
ε_{tt}	Transient transverse strain in geosynthetics (%)
ε_{tv}	Transient vertical strain of ballast layer (%)
ε_v	Vertical strain of ballast layer (%)

7. ACKNOWLEDGEMENTS

The authors are grateful to the CRC for Rail Innovation (established and supported under the Australian Government's Cooperative Research Centres program) for funding a significant part of this research through project no. R3.106 entitled 'Integrated Ballast-Formation-Track Design and Analysis including the Implications of Ballast Fouling and High Impact Loads' and project no. R3.117 entitled 'Track Design and Analysis for Impact and Cyclic Loads - Singleton Field Study'. The authors express their sincere thanks to Australian Research Council, RailCorp (Sydney), ARTC and Aurizon Holdings Limited (previously known as QR National), for their continuous support. The assistance of Dr Pongpipat Anantanasakul (Lecturer, Mahidol University, Thailand) during his stay at University of Wollongong as a part of his postdoctoral research programme is gratefully acknowledged. A number of past research students of the first author, namely, Dr Ngoc Trung Ngo, Dr Nayoma Chulani Tennnakoon, and Dr Syed Khaja Karimullah Hussaini have also contributed to the contents of this paper through their research work. The authors would like to thank Alan Grant, Cameron Neilson and Ian Bridge of the University of Wollongong for their technical assistance throughout the period of this study. The on-site assistance provided by Carol Bolam, Tony Miller, and Darren Mosman of Hunt8r Alliance (Newcastle) and David Williams of ARTC (Newcastle) is appreciated.

More elaborate details of the contents discussed in this paper can be found in previous publications of the first author and his research students in ASCE, Géotechnique and Canadian Geotechnical Journal, since mid 1990's.

8. REFERENCES

Anderson, W. F., and Fair, P. (2008) "Behaviour of railroad ballast under monotonic and cyclic loading", Journal of Geotechnical and Geoenvironmental Engineering ASCE, 134, Issue 3, pp 316-327.

Ashmawy, A. K., and Bourdeau, P. L. (1995) "Geosynthetic-reinforced soils under repeated loading: a review and comparative design study", Geosynthetics International, 2, Issue 4, pp 643-678.

Ashpiz, E. S., Diederich, R., and Koslowski, C. (2002) "The use of spunbonded geotextile in railway track renewal on the St. Petersburg-Moscow line", Proceedings of the 7th Int. Conference on Geosynthetics, Nice, France, pp 14-19.

Aursudkij, B. (2007) "A laboratory study of railway ballast behaviour under traffic loading and tamping maintenance", PhD thesis, University of Nottingham, UK.

Australian Rail Track Corporation (ARTC) (2006a) RCP-01: Standard for Earthworks Construction Procedures, Australian Rail Track Corporation Limited, Newcastle, Australia.

Australian Rail Track Corporation (ARTC) (2006b) TDS-12: Standard for Formation Capping Material, Australian Rail Track Corporation Limited, Newcastle, Australia.

Australian Rail Track Corporation (ARTC) (2007a) ETA-04-01: Ballast Specifications, Australian Rail Track Corporation Limited, Newcastle, Australia.

Australian Rail Track Corporation (ARTC) (2007b) TDS-08: General Standards for Formation and Earthworks, Australian Rail Track Corporation Limited, Newcastle, Australia.

Australian Standard (AS) (2012) 1141.3.1: Methods for sampling and testing aggregates Method 3.1: Sampling-Aggregates, Standards Australia, Sydney, Australia.

Bathurst, R. J., and Raymond, G. P. (1987) "Geogrid Reinforcement of Ballasted Track" Transportation Research Record, 1153, pp 8-14.

Brown, S. F., Kwan, J., and Thom, N. H. (2007) "Identifying the key parameters that influence geogrid reinforcement of railway ballast", Geotextiles and Geomembranes, 25, Issue 6, pp 326-335.

Brown, S. F., and Selig, E. T. (1991) "The design of pavement and rail track foundations", cyclic loading of soils: from theory to design, Blackie and Son Ltd, New York, pp 249-305.

Chen C., McDowell G. R., and Thom, N. H. (2012) "Discrete element modelling of cyclic loads of geogrid-reinforced ballast under confined and unconfined conditions", Geotextiles and Geomembranes, 35, Issue 12, pp 76-86.

Dahlberg, T. (2006) Track Issues, Handbook of Railway Vehicle Dynamics, 143-179. Taylor & Francis Group.

Dombrow, W., Huang, H., and Tutumluer, E. (2009) "Comparison of coal dust fouled railroad ballast behavior-granite vs. limestone", In E. Tutumluer & I. Al-Qadi (Eds.), Proceedings of Eighth International Conference on the Bearing Capacity of Roads, Railways, and Airfields, London: Taylor and Francis Group, pp 1349-1357.

Esveld, C. (2009) The significance of track resilience. In European Rail Review Digital News Issue 10, p 14-20.

Feldman, F. and Nissen, D. (2002). "Alternative testing method for the measurement of ballast fouling." Conference on Railway Engineering. Wollongong, RTSA.

Fernandes, G., Palmeira, E. M., and Gomes, R. C. (2008) "Performance of geosynthetic-reinforced alternative sub-ballast material in a railway track", Geosynthetics International, 15, Issue 5, pp 311-321.

Ferreira, P. A., and López-Pita, A. (2013) "Numerical modeling of high-speed train/track system to assess track vibrations and settlement prediction", Journal of Transportation Engineering ASCE 139, Issue 3, pp 330-337.

Fischer, S., and Horv′at, F. (2011) "Substructure stabilization of ballast bedded railway tracks with geogrids", Hungarian Journal of Industrial Chemistry Veszpre′m, 39, Issue 1, pp 101-106.

Han, X., and Selig, E. T. (1997) "Effects of fouling on ballast settlement", Proceedings of the Sixth International Heavy Haul Conference, Cape Town, South Africa, pp 257-268.

Huang, H., Tutumluer, E., and Dombrow, W. (2009) "Laboratory characterisation of fouled railroad ballast behavior", Transportation Research Record: Journal of the Transportation Research Board, No. 2117. Washington, DC.

Indraratna B., and Nimbalkar S. (2013) "Stress-strain degradation response of railway ballast stabilized with geosynthetics", Journal of Geotechnical and Geoenvironmental Engineering ASCE, 139, Issue 5, pp 684-700.

Indraratna, B., and Salim, W. (2003) "Deformation and degradation mechanics of recycled ballast stabilised with geosynthetics", Soils and Foundations, 43, Issue 4, pp 35-46.

Indraratna, B., Hussaini, S. K., and Vinod J. S. (2011a) "On the shear behaviour of ballast-geosynthetic interfaces", Geotechnical Testing Journal ASTM, 35, Issue 2, pp 1-8.

Indraratna, B., Khabbaz, H., Salim, W., and Christie, D. (2006). "Geotechnical properties of ballast and the role of geosynthetics in rail track stabilization", Ground Improvement, 10, Issue 3, pp 91-101.

Indraratna, B., Lackenby, J., and Christie, D. (2005) "Effect of confining pressure on the degradation of ballast under cyclic loading", Géotechnique, 55, Issue 4, pp 325-328.

Indraratna, B., Ngo, N. T., and Rujikiatkamjorn, C. (2013) "Studying the deformation of coal fouled ballast stabilised with geogrid under cyclic load", J. of Geotechnical & Geoenvironmental Engineering, ASCE DOI: 10.1061/(ASCE)GT.1943-5606.0000864.

Indraratna, B., Nimbalkar, S., and Rujikiatkamjorn, C. (2012a) "Track stabilisation with geosynthetics and geodrains, and performance verification through field monitoring and numerical modeling", International Journal of Railway Technology 1, Issue 1, pp 195-219.

Indraratna, B., Nimbalkar, S., and Rujikiatkamjorn, C. (2012b) "Future of Australian rail tracks capturing higher speeds with heavier freight", Sixteenth annual Symposium of Australian Geomechanics Society, Advances in Geotechnics of Roads and Railways, Sydney Chapter, 10 October 2012, Sydney, Australia, pp 1-24.

Indraratna, B., Nimbalkar, S., and Tennakoon, N. (2010b) "The behaviour of ballasted track foundations: track drainage and geosynthetic reinforcement", GeoFlorida 2010, ASCE Annual GI Conference, February 20-24, 2010, West Palm Beach, Florida, USA, pp 2378-2387.

Indraratna, B., Nimbalkar, S., Christie, D., Rujikiatkamjorn, C., and Vinod, J. S. (2010a) "Field assessment of the performance of a ballasted rail track with and without geosynthetics", Journal of Geotechnical and Geoenvironmental Engineering ASCE, 136, Issue 7, pp 907-917.

Indraratna, B., Salim, W., and Rujikiatkamjorn, C. (2011b) Advanced Rail Geotechnology – Ballasted Track: CRC Press/Balkema.

Indraratna, B., Shahin, M. A., and Salim, W. (2007) "Stabilising granular media and formation soil using geosynthetics with special reference to Railway engineering", Ground Improvement, 11, Issue 1, pp 27-44.

Jeffs, T., and Tew, G. P. (1991) "A review of track design procedures: sleepers and ballast", Vol. 2, Railways of Australia BHP Research, Melbourne Laboratories, Melbourne, Australia.

Jenkins, H. M., Stephenson, J. E., Clayton, G. A., Morland, J. W., and Lyon, D. (1974) "The effect of track and vehicle parameters on wheel/rail vertical dynamic forces", Railway Engineering Journal, 3, pp 2-16.

Kempfert, H. G., and Hu, Y. (1999) "Measured dynamic loading of railway underground", Proceedings of the 11th Pan-American Conference on Soil Mechanics and Geotechnical Engineering, International Society for Soil Mechanics, Brazil, pp 843-847.

Lackenby, J., Indraratna, B., McDowell, G., and Christie, D. (2007) "Effect of confining pressure on ballast degradation and deformation under cyclic triaxial loading", Géotechnique, 57, Issue 6, pp 527-536.

Li, D., and Davis, D. (2005) "Transition of Railroad Bridge Approaches" Journal of Geotechnical and Geoenvironmental Engineering ASCE, 131, Issue 11, pp 1392-1398.

McDowell, G. R., Harireche, O., Konietzky, H., Brown, S. F., and Thom, N. H. (2006) "Discrete element modelling of geogrid-reinforced aggregates", Proceedings of the Institution of Civil Engineers - Geotechnical Engineering 159, Issue 1, pp 35-48.

Montanelli, F., and Recalcati, P. (2003) "Geogrid reinforced railway embankment: design concepts and experimental test results", In "IABSE Symposium for Structures for High-Speed Railway Transportation," (2003) Antwerp, 27-29 August.

Nimbalkar, S., Indraratna, B., Dash, S. K., and Christie, D. (2012) "Improved performance of railway ballast under impact loads using shock mats", Journal of Geotechnical and Geoenvironmental Engineering ASCE, 138, Issue 3, pp 281-294.

Rail Infrastructure Corporation (RIC) (2001a) Specification for supply of aggregates for ballast. TS 3402, Sydney, Australia.

Raymond, G. P. (2002) "Reinforced ballast behaviour subjected to repeated load", Geotextiles and Geomembranes, 20(1): 39-61.

Raymond, G. P., and Bathurst, R.J. (1994) "Repeated-load response of aggregates in relation to track quality index", Canadian Geotechnical Journal, 31, pp 547-554.

RCA Australia (2008) Geotechnical Investigation Report for Minimbah Bank Third Track. RCA Australia, Newcastle, Australia.

Selig, E. T., and Waters, J. M. (1994) Track Geotechnology and Substructure Management, Thomas Telford, London. Reprint 2007.

Shenton, M. J. (1975) Deformation of railway ballast under repeated loading conditions. Railroad Track Mechanics and Technology (Kerr ed.), Princeton University, pp 387-404.

Shin E. C., Kim D. H., and Das B. M. (2002) "Geogrid-reinforced railroad bed settlement due to cyclic load", Geotechnical and Geological Engineering, 20, Issue 3, pp 261-271.

Tennakoon, N. (2013) "Geotechnical study of engineering behaviour of fouled ballast", PhD Thesis, University of Wollongong.

Tennakoon, N., Indraratna, B., Rujikiatkamjorn, C., Nimbalkar, S., and Neville, T. (2012) "The Role of Ballast Fouling Characteristics on the Drainage Capacity of Rail Substructure", ASTM Geotechnical Testing Journal, 35, Issue 4, pp 1-12.

Tutumluer, E., Dombrow, W., and Huang, H. (2008) "Laboratory Characterization of Coal Dust Fouled Ballast Behavior", AREMA 2008 Annual Conference & Exposition. Salt Lake City, UT, USA.